Comparison of Multivariable Control Algorithms for Load-sensing Electro-hydraulic Servo System

Tsonyo Slavov, Alexander Mitov, Jordan Kralev, Ilcho Angelov

***Abstract* — Comparison of two embedded multivariable control algorithms based on advanced control techniques - LQG and H_∞ is done. The controllers are designed to control a load-sensing electro-hydraulic system for driving the power steering of modern generation mobile machinery. The authors have developed the two controllers separately in previous works, where their theoretical and experimental research was performed. The purpose of the present article is to compare the two controllers in terms of physical experiment and numerical simulation, and on the basis of their comparison to be analyzed their workability and control performance. The comparison is made on the basis of several indices defined the control system performance in both the time domain and the frequency domain. Simulation and real time experiments show the advantages of H-infinity controller.**

***Index Terms* — Electro-hydraulic, H_∞, load-sensing, LQG, servo**

I. INTRODUCTION

Two main types of control techniques are used to control electro-hydraulic servo systems. The first type is based on conventional control laws, such as PID and their variants [1,2]. The second type are advanced control techniques including - LQG, H∞ and μ [3,4,5,6,7].

In electro-hydraulic servo systems, which do not have cross-feedback between the channels, classical PID control laws are most often used, which solve the control task reaching the desired performance.

In the electro-hydraulic servo systems for power steering of mobile machinery to precise motion control of the wheels and to overcome resistance forces acting on the steered axle it is needed to use various physical quantities for feedbacks. General difficult in such multivariable systems is that the conventional embedded controllers cannot ensure control performance due to presence of cross-connections between the multivariable plant channels. Thus, controllers designed on the basis of multivariable plant model are more appropriate.

In addition, in the case of a remote control via a microcontroller, the behavior of the machine strongly depends on the embedded control algorithm. In this case the control performance can be achieved by using a multivariable plant model instead several single input single output models. However, obtaining of such models are more complicated problem. At the other hands, a compromise between the complexity and accuracy of the model is always required. Complex models are usually suitable for analyzing the dynamics of the system, but are inconvenient for the design of embedded controllers.

Two approaches are most often used to determine a mathematical model of an electrohydraulic servo system - physical modeling or identification. Physical modeling requires in-depth knowledge of the structure of the plant and the relevant physical parameters (flow-pressure characterristics, hydraulic resistances, closed volumes, geometry of the control edges of spools). Due to the lack of such a priori information, a numerical model obtained through an identification procedure based on experimental data is studied [8]. Another reason for this approach is the ability to derive a noise model that can be used to design an optimal Kalman filter [9].

The major problem in designing a LQG controller on the basis of model obtained by identification is that the state variables are not measurable and they have not physical sense in general [10]. The absence of information for the states can be fulfilled by stochastic state observer. The Kalman filter is optimal state observer in case of linear plant model and Gaussian signals. This means that noise model should be known. One of the advantages of models obtained by identification is that the noise model is estimated along with process model. Moreover, to provide precise reference tracking, an extended LQG controller with integral action is synthesized.

The H∞ controller has also been designed based on the identified model by selecting appropriate manipulated signals and performance indicators, together with respective weighting filters. Selection of the weighting filters is achieved by observing the requirements for good load disturbance attenuation in the low frequency band and acceptable controller gain in the high frequency band associated with the sensor noise amplification in the actuators. The H∞ synthesis is carried by selecting an upper bound for the H∞ norm of the closed-loop interconnection between external disturbances and the performance indicators for a parametrized controller family.

The main purpose of this article is to present the results of the comparison of two types advanced control algorithms – LQG and H∞. The both embedded controllers have been designed and studied separately in previous works of the authors. Based on the present comparison, an analysis of their workability and control performance was provided.

II. PLANT MODELING

In previous work, we develop a new test setup for realization of laboratory Load-sensing servo system applicable for power steering mobile machinery [11]. The hydraulic circuit diagram of the system implemented on the test setup is depicted in Fig.1. The detailed description of the system used for the experimental studies was made in [11,12].

https://doi.org/10.47978/TUS.2021.71.02.008

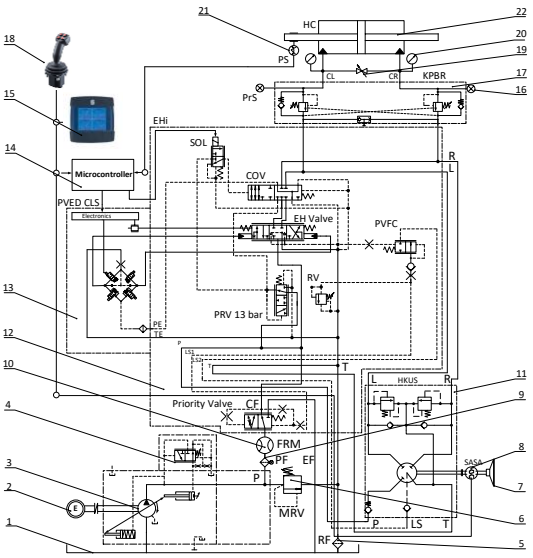

Fig. 1. Hydraulic circuit diagram of test rig for LS servo position system.

The model of load sensing electrohydraulic servo system can be obtained by analytical modelling approach or system identification approach [8]. In our case, due to the lack of a priori information about parameters of internal devices of system, the identification approach is used. The main advantages of models determined by so called "black box" approach are that the description of the all devices like noises, actuators and sensor dynamics are obtained. The identification procedure applied to the electrohydraulic load sensing servo system is given in details in [11]. Here we shortly present the obtained plant model. The linear model that describes sufficiently well dynamics of electro-hydraulic steering system is given by

$$\begin{aligned} x(k+1) &= Ax(k) + Bu(k) + Ke(k) \\ y(k) &= Cx(k) + Du(k) + e(k) \end{aligned} \tag{1}$$

where $x = \begin{bmatrix} x_1 & x_2 & x_3 & x_4 \end{bmatrix}^T$ is a state vector, u is a control signal (voltage applied to the control input of PVE), $y = \begin{bmatrix} y_{LVDT} & y_{pos} \end{bmatrix}^T$ is output signals (y_{LVDT} is output of LVDT sensor and y_{pos} is a cylinder piston position), $e(k) = \begin{bmatrix} e_1 & e_2 \end{bmatrix}^T$ is a residual vector, e_1 is residual respect to the LVDT while e_2 is residual respect to cylinder positon position. The matrices A, B, C, D and K take the values

$$\begin{aligned} A &= \begin{pmatrix} 0 & 1 & 0 & 0 \\ -2.1432 & 2.1207 & 1.4618 & -1.4624 \\ 0 & 0 & 0 & 1 \\ -0.3563 & -0.3524 & 0.0464 & 0.9532 \end{pmatrix}, \\ B &= 10^{-5} \begin{pmatrix} 0.0231 \\ 0.4533 \\ 0.2308 \\ -0.4971 \end{pmatrix}, C = \begin{pmatrix} 1 & 0 & 0 & 0 \\ 0 & 0 & 1 & 0 \end{pmatrix}, \\ D &= \begin{pmatrix} 0 \\ 0 \end{pmatrix}, K = \begin{pmatrix} 1.5999 & -0.0031 \\ 1.7777 & -0.0084 \\ -0.5023 & 0.9847 \\ -1.4377 & 0.9866 \end{pmatrix} \end{aligned} \tag{2}$$

Model parameters in equation (2) are determined by model predictive error method. In estimation, the observable canonical form is used..

III. LQG AND H_∞ CONTROLLER DESIGN

The block schemes of control systems with designed LQG controller and H_∞ controllers are shown in Fig. 2 and Fig. 3 respectively. The detailed description of LQG and H_∞ controllers design is given in [13] and [14]. Here for comparison purpose we give only short description of controller synthesis.

In the LQG system, the piston position tracking is provided by integral action of controller. The controller design is done on the basis of model (1), which is extended with additional integral state.

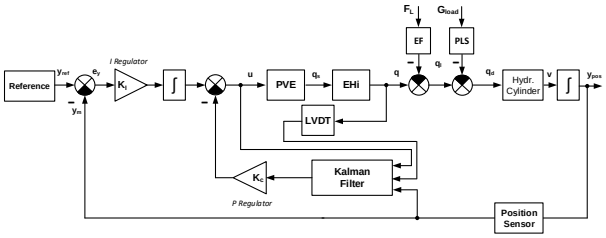

Fig. 2. Block scheme of closed-loop system based on the. LQG controller.

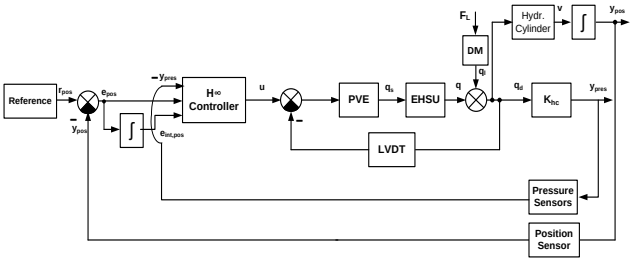

Fig. 3. Block scheme of closed-loop system based on the. H_∞ controller

The extended model used in LQR controller design is given by

$$\begin{aligned} \bar{x}(k+1) &= \bar{A}\bar{x}(k) + \bar{B}u(k) + \bar{G}y_{ref}(k), \\ y(k) &= \bar{C}\bar{x}(k), \end{aligned} \tag{3}$$

where

$$\bar{x}(k) = \begin{vmatrix} x_i(k) \\ x(k) \end{vmatrix}, \bar{A} = \begin{vmatrix} 1 & -T_s C_2 \\ 0_{4\times 1} & A \end{vmatrix}, \bar{B} = \begin{vmatrix} 0 \\ B \end{vmatrix}, \bar{C} = \begin{vmatrix} 0_{2\times 1} & C \end{vmatrix}, \bar{G} = \begin{vmatrix} T_s \\ 0_{4\times 1} \end{vmatrix}.$$

C_2 is the second row of matrix C and $x_i(k)$ is discrete time integral of piston position error. The optimal control law is obtained as

$$u(k) = -\bar{K}\bar{x}(k), \bar{K} = [-K_i \quad K_c], \tag{4}$$

where

$K_c = \begin{bmatrix} -1407 & 868 & 1203 & -1247 \end{bmatrix}$ and $K_i = 14$

for weighting matrices

$$Q = \begin{bmatrix} 20 & 0 \\ 0 & C^T \begin{vmatrix} 100 & 0 \\ 0 & 0.1 \end{vmatrix} C \end{bmatrix}, R = 0.1 \tag{5}$$

The large values of the feedback gains is due to physical unit of millivolts used to set up the control voltage.

To form the control law (6), the estimate $\hat{x}(k)$ of $x(k)$ are required. They are obtained by Kalman filter [7]

$$\begin{aligned}\hat{x}(k+1) &= A\hat{x}(k) + Bu(k) + \\ K_f\,(y(k+1) &- CBu(k) - CA\hat{x}(k))\end{aligned}, \tag{6}$$

where gain matrix K_f is evaluated by *MATLAB*® function *kalman* applied for model (1)-(2). The obtained gain matrix is

$$K_f = \begin{bmatrix} 1.6 & 1.8 & -0.5 & -1.4 \\ 0 & 0 & 0.98 & 0.99 \end{bmatrix}^T \tag{7}$$

As can be seen the first output signal (cylinder piston position) affects to the estimates of the 4 states and the LVDT signal affects mainly to the estimates of the x_3 and x_4.

The obtained 4-rd order model is used also for H_∞ controller [14] design according to scheme presented in Fig. 4. The design criteria is mixed *S/KS* sensitivity.

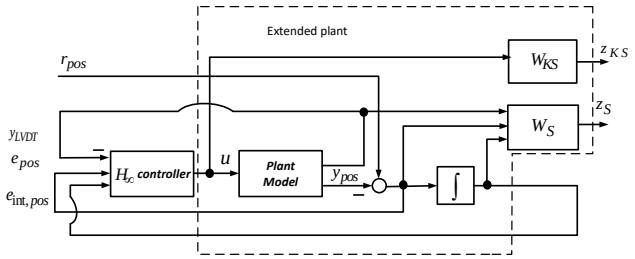

Fig. 4. Scheme for H∞ controller design.

The control signal of H_∞ controller is formed by

$$u = Ky_c, \tag{8}$$

where $y_c = \begin{pmatrix} -y_{LVDT} & e_{pos} & e_{\text{int},pos} \end{pmatrix}^T$ is the output vector with signals that are used in feedback and $K_c = \begin{pmatrix} K_1 & K_2 & K_3 \end{pmatrix}$ is the controller matrix. The performance output $z = \begin{pmatrix} z_S & z_{KS} \end{pmatrix}^T$ is related to the reference signal r_{pos} by

$$\begin{pmatrix} z_s \\ z_{KS} \end{pmatrix} = W_{zr} r, \tag{9}$$

where W_{zr} is the transfer matrix between performance outputs and position reference. The performance output respect to sensitivity matrix is represented as

$$z_S = \begin{pmatrix} z_{LVDT}, z_{pos}, z_{\text{int}} \end{pmatrix}^T \tag{10}$$

where z_{LVDT} is weighted LVDT sensor output, z_{pos} is weighted position error and z_{int} is weighted integral of the position error. The H_∞ controller design problem is to find a controller which stabilizes closed loop and minimizes criteria

$$\min_{K_{stibilizing}} \left\| W_{zr} \right\|_\infty \tag{11}$$

Exactly minimization of objective function (11) is difficult. Instead minimization of (11), design procedure finds the suboptimal H_∞ controller which provides

$$\left\| \left[W_{zr} \right] \right\|_\infty < \gamma\ , \tag{12}$$

where γ is a positive scalar. Value of γ smaller than 1 means that obtained H_∞ controller satisfies prescribed by weighting functions W_S and W_{KS} performance criteria. The controller design is performed for various weighting functions. On the basis of closed loop system simulation and our previous experience the performance functions are chosen as

$$W_S = diag\left(0.1 \quad 0.005 \quad Z\left[\frac{0.8(0.1s+1)}{0.5s+1} \right] \right), W_{KS} = 0.08$$

where $Z[\bullet]$ denotes Z-transformation. As a result we obtain stabilizing H_∞ controller of 7-th order and value of γ is 0.9567

IV. Performance Comparison via Simulation Experiments

In this section we compare the frequency and time domain properties of control system based on the LQG controller (denoted by LQG system) and control system based on the H_∞ controller (denoted by H_∞ system). In Fig. 5 the output sensitivities respect to cylinder piston position are presented. In Fig.6 complementary sensitivities and plant amplitude frequency response are introduced. The sensitivity of control signal respect to noise are depicted in Fig.7.

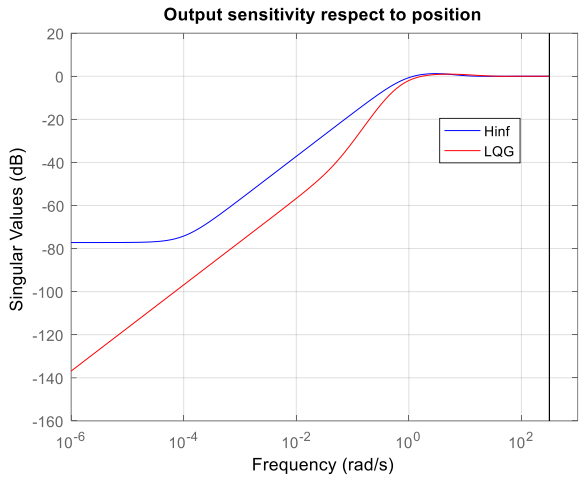

Fig. 5. Output sensitivities respect to cylinder piston position

It is seen that the both system will suppress sufficiently well load disturbance (LQG system will reduce 1000 times efect of disturbance with frequency of 0.01*rad/s* and H_∞ system will reduce 100 times effect of the same disturbance). The bandwidth ω_{BT} of H_∞ system is wider than one of LQG system. The both systems extend sufficiently plant bandwidth. The sensitivity of control action to noises is acceptable for both systems, but it is seen that the H_∞ system will increase noises more than LQG system.

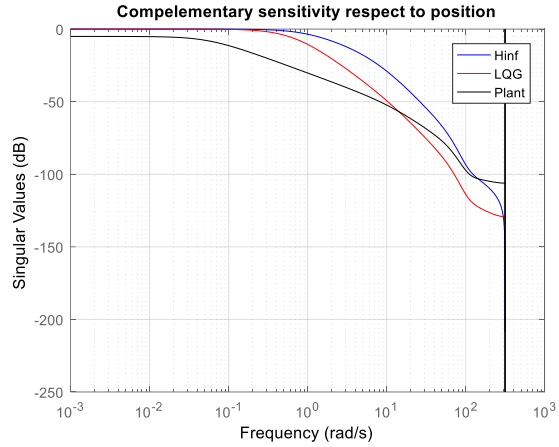

Fig. 6. Complementary sensitivities and plant frequency response respect to cylinder piston position

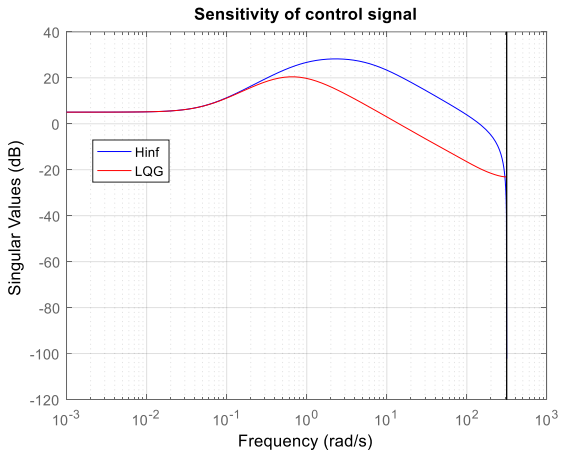

Fig. 7. Sensitivities of control signals to noises

The step response of H_∞ system is 2 times faster than one of the LQG system. The both system has aperiodic transient responses. The control signals has acceptable for and do not exceed maximum value of 5 V.

The quantitative analysis in frequency and time domain is performed on the basis of indices:

– H-infinity norm of output sensitivity

$$M_s = \left\| S(j\omega) \right\|_\infty , \qquad (13)$$

where $\left| S(j\omega) \right|$ is complementary sensitivity of closed loop system.

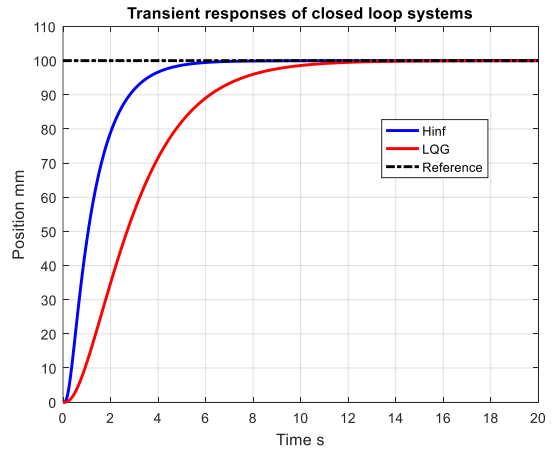

Fig. 8. Transient responses of closed loop systems respect to position

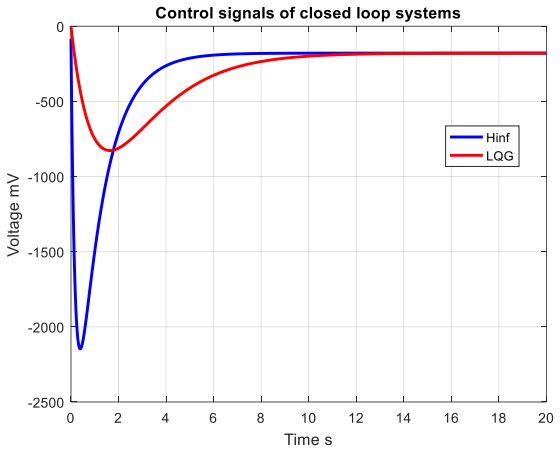

Fig. 9. Control signals of closed loop systems

– Closed loop bandwidth ω_{BT}. It is defined as frequency at which complementary sensitivity $\left| T(j\omega) \right|$ respect to cylinder piston position crosses line -3db from above.

– Overshoot

$$\sigma = \frac{y_{pos,\max} - y_{pos}(\infty)}{y_{pos}(\infty)} 100[\%], \qquad (14)$$

where $y_{pos,\max}$ is the first peak of the transient response respect to cylinder piston position and $y_{pos}(\infty)$ is its steady state value

– Settling time t_s. It is defined as the minimum period of time after which the cylinder piston position remains within 5 percent of its steady-state value.

– Square root of integral error respect to cylinder piston position

$$J_e = \sqrt{\frac{1}{N}\sum_{i=0}^{N-1}(r(i) - y_{pos}(i))^2} \qquad (15)$$

The values of above described indices for both control systems are given in Table 1

TABLE I
PERFORMANCE INDICES OBTAINED BY SIMULATION EXPERIMENT

	M_S [Db]	ω_{BT} [rad/s]	σ%	t_{st} [s]	J_e
LQG	0.98	0.4	0	12	31.94
H_∞	1.2	0.8	0	6	20.27

It is seen that the settling time for H_∞ system is 2 times smaller than one for LQG system. The index (15) for H_∞ system is 50% smaller than one for LQG system.

V. PERFORMANCE COMPARISON VIA TEST RIG EXPERIMENT

The schematic diagram of the developed by authors extended real-time computation environment, which allows fast prototyping of control algorithms for load sensing electro-hydraulic servo system is presented in Fig.10 [13].

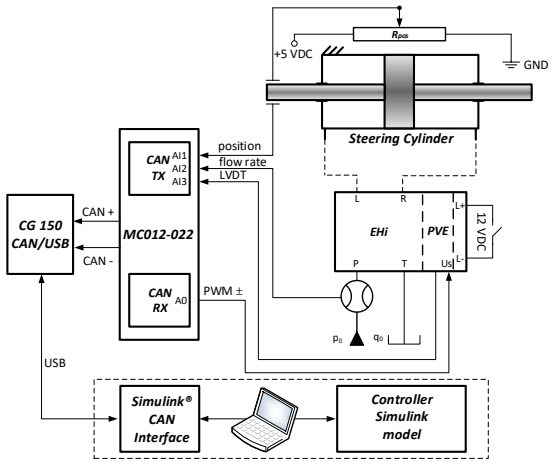

Fig. 10. Computational system for fast prototyping of controllers.

Key blocks in diagram in Fig.10 are "Controller Simulink model" and "Simulink CAN Interface". The first one is used for realization of state space controller and the second is used for CAN communication between Simulink model and microcontroller MC012-022r. The block "Controller Simulink model" is presented in details in Fig.11

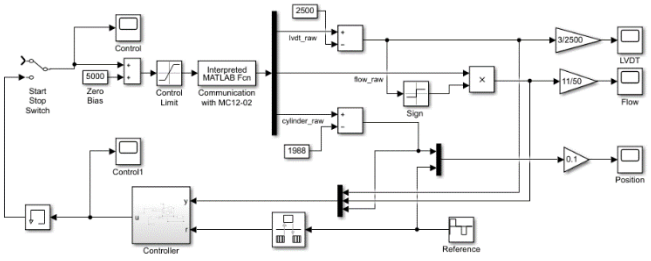

Fig. 11. Simulink® diagram for implementation of designed controller.

A MATLAB® function block is responsible for the communication on a CAN network where the embedded controller MC012-022 is connected.

In the MATLAB environment the CAN channel is accessed through a dedicated instance of the CAN class initialized with

a = canChannel("Kvaser"," 1",1)

where "Kvaser" is the name of the USB-CAN communication driver automatically enumerated in the MATLAB. Then a CAN message object is instantiated with

m = canMessage(124,false,8)

where the address 124 of the slave device is specified. The slave in this case is the MC12 microcontroller. The second parameter is whether an extended CAN frame is employed which is not the case in our experiments. The last parameter is the length of the dataframe. The communication channel is configured to work at 1 megabit per second with

a.configBusSpeed(1000000).

The high speed is required to allow a small sampling intervals during the real-time operation of the designed controller. The communication is initiated with

a.start()

method, which opens the connection on CAN network and acquired messages are buffered in the driver memory. The communication function code executed at each simulation step in the MATLAB function block is presented in the Fig. 12.

```
function y = can_fcn(u)
  c = evalin('base','a');
  msg = evalin('base','m');
  bufu = uint16(u);
  msg.Data(1) = uint8(bufu);
  msg.Data(2) = uint8(bitshift(bufu,-8));
  c.transmit(msg);
  y = evalin('base','ylast');
  while (c.MessagesAvailable < 2)
  end
  for ind = 1:c.MessagesAvailable
    buf = c.receive(1);
    if buf.ID == 123
      dat = uint16(buf.Data);
      y(1) = double(bitor(dat(1),bitshift(dat(2),8)));
      y(2) = double(bitor(dat(3),bitshift(dat(4),8)));
      y(3) = double(bitor(dat(5),bitshift(dat(6),8)));
      assignin('base','ylast',y);
    end
  end
```

Fig. 12. Source code of real-time communication algorithm

The first step is to send the input signal u to the microcontroller. The datatype of this input signal is 16 bit signed integer reflecting the applied voltage to the PVE actuator in millivolts. The input signal is represented as two 8 bit variables mapped into the msg.Data array with the help of MATLAB bitshift command. The constructed message with the control signal is transmitted over the CAN channel with

c.transmit(msg)

statement. After the transmission of the message the host waits for a response from the controller which should come after one sampling interval Ts. Since the microcontroller is the only device connected on the CAN bus a number of available messages is monitored. During that period of waiting for messages the execution of the Simulink diagram is blocked and the controller waits for the next sample of data from the microcontroller. The reason to check for two messages available instead of a single one is that the message sent from the host is also acquired as an available message. Hence, when the target message count is reached, all messages are received and scanned for the host ID, which is set to 123. When the host id is matched the data field of the message is decoded using bitwise arithmetic. The message from the microcontroller contains 3 variables (spool position, flow rate and the cylinder position), which are represented with 16 bit signed integer numbers.

In Fig. 13 and Fig. 14 transient responses of both control systems respect to cylinder piston position and LVDT sensor signal are presented. In Fig. 15 the results for control signals are depicted.

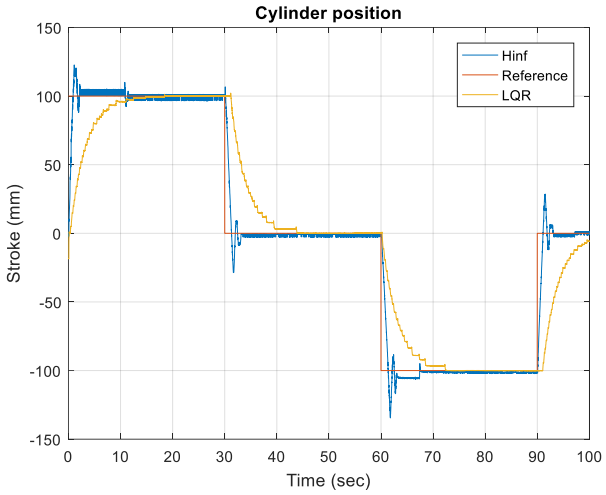

Fig. 13. Transient responses of closed loop systems respect to position

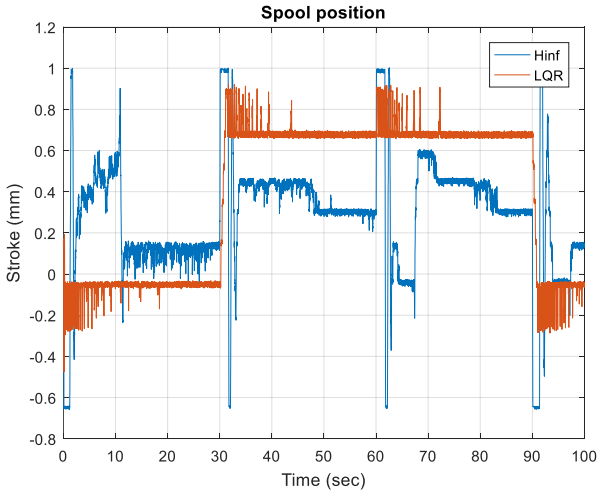

Fig. 14. Transient responses of closed loop systems respect to LVDT

In Table 2 some of performance indices in time domain are calculated for real time experiments.

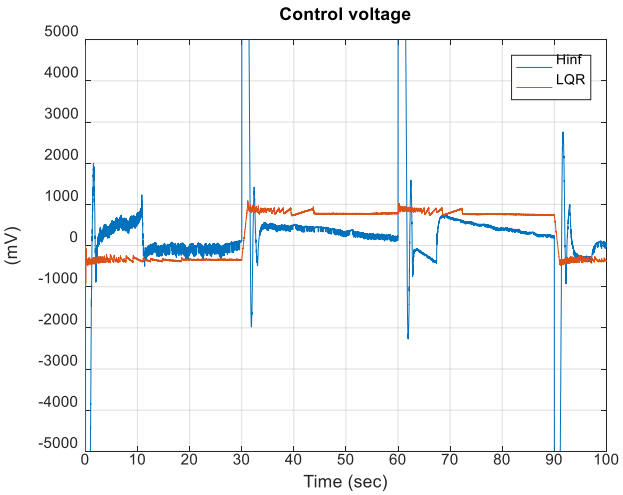

Fig. 15. Control signals

[i]TABLE 2
PERFORMANCE INDICES OBTAINED BY REAL EXPERIMENT

	$\sigma\%$	t_{st} [s]	J_e
LQG	0	9.2	859.12
H_∞	18	2.2	197.88

It is seen that the settling time and index (14) for H_∞ system is more than 4 times smaller than ones for LQG system, but the transient response of H_∞ system has overshoot of 18%, which is admissible for heavy duty mobile machinery. The control signal of H_∞ system for short time achieves limit of 5 *V*. The explanation is that the sensitivity of control signal to noises for H_∞ system is higher than one for LQG system (see Fig.7).

VI. CONCLUSION

The article presents comparative analysis of performance of two embedded control systems based on LQG and H_∞ algorithms. The controllers are designed to control a load-sensing electro-hydraulic system for driving the power steering of modern generation mobile machinery. The main purpose is comparison of control performance via physical experiment and numerical simulation. The presented results approve workability and performance of both systems. The calculated indices in time and frequency domains show the advantage of system based on the H_∞ controller.

REFERENCES

[1] Mitov, Al., J. Kralev, Il. Angelov, Cascade control algorithm of test bench for studying load-sensing electrohydraulic steering systems, BulTrans-2018, Proceedings Matec Web of Conference, ISSN 2261-236X, 2018, https://doi.org/10.1051/matecconf/201823402006

[2] Merrit H 1967 Hydraulic Control Systems (John Wiley & Sons, Inc.)

[3] Slavov Ts, Mitov Al, Kralev J 2020 Advanced Embedded Control of Electrohydraulic Power Steering System Cybernetics and Information Technologies 20(2) 105-121, https://doi.org/10.2478/cait-2020-0020

[4] Goodwin G C, Graebe S F and Salgado M E 2001 Control System Design (Prentice-Hall Inc.)

[5] Rigatos G, Zervos N, Abbaszadeh M, Pomares J nd Wira P 2020 Non-linear optimal control for multi-DOF electro-hydraulic robotic manipulators IET Cyber-Systems and Robotics 2(2) 96-106, https://doi.org/10.1049/iet-csr.2020.0003

[6] Rigatos G, Abbaszadeh M, Siano P and Cuccurullo G 2020 Nonlinear optimal control of electro-hydraulic actuators IFAC Journal of Systems and Control 15(100130) 1-10, DOI: 10.1016/j.ifacsc.2020. 100130

[7] Guo Q, Yu T and Jiang D 2015 Robust H∞ positional control of 2-DOF robotic arm driven by electro-hydraulic servo system ISA Transactions, 59, 55–64, https://doi.org/10.1016/j.isatra.2015.09.014

[8] Ljung L 1999 System Identification: Theory for the User (Prentice-Hall Inc.)

[9] Grewal M.S., Andrews. A.P. Kalman Filtering: Theory and Practice with MATLAB®, 4th ed. John Wiley & Sons, Inc., New York, ISBN 978-1-118-85121-0, 2015

[10] Franklin, J.D. Powell, M.L. Workman. Digital Control of Dynamic Systems, 3rd ed. Addison Wesley Longman, Inc., Menlo Park, CA, ISBN 0-201-33153-5, 1998.

[11] Mitov Al, Slavov Ts, Kralev J, Angelov Il 2021 Identification of Electro-Hydraulic Load-Sensing Servo System. 20th Int. Scientific Conf. Engineering for Rural Development (Jelgava), ISSN 1648-1654, https://doi.org/10.22616/ERDev.2021.20.TF356

[12] Danfoss Inc., Steering, EHi steering valve, Technical Information, BC00000379en-US0202, 2018.

[13] Mitov A., Kralev J., Slavov T. and I. Angelov, LQG Control of Load-Sensing Electro-hydraulic Servo System, 2021 10th Mediterranean Conference on Embedded Computing (MECO), 2021, pp. 1-6, doi: 10.1109/MECO52532.2021.9460296.

[14] Mitov, A., Kralev, J., Slavov, T., Angelov, I. H_∞ control of load-sensing electro-hydraulic servo system. IOP Conference Series: Materials Science and Engineering, 2021 (in press), https://doi.org/10.1109/MECO52532.2021.9460296